The effect of conical dimple spacing on flow structure and heat transfer characteristics of internal flow using CFD

O Yemin[1], M Wae-Hayee[1`*], P Narato[1], K Yerane[1], K Abdullah[2] and C Nuntadusit[1]

[1] Energy Research Centre and Department of Mechanical Engineering, Faculty of Engineering, Prince of Songkla University, Hat Yai, Songkhla 90112, Thailand

[2] Department of Energy and Thermofluid Engineering, Faculty of Mechanical and Manufacturing Engineering, UniversitiTun Hussein Onn Malaysia, Johor, Malaysia

E-mail: wmakatar@eng.psu.ac.th.

Abstract. In the present study, heat transfer and flow characteristics simulations over the surface of conical dimple were investigated. Single dimple row with inline arrangement was formed on the internal surface of the 3-D rectangular wind tunnel model. The air flow was perpendicular to the centre line of every dimple and the printed diameter of dimples on the surface was D=26.4mm. The depth of dimple on the surface of wind tunnel was H/D=2. The space between dimple-to-dimple was varied for S/D=1.125, 1.25,1.5, and 2. The Reynold number based on the hydraulic diameter of internal air flow was 20,000 depending on the wind tunnel hydraulic diameter. The numerical computation was applied with a Shear Stress Transport (SST) k-ω turbulence model. The average Nusselt number for the S/D=1.125 case is the highest. When the spacing becomes increase, the value of average Nusselt number tends to decrease.

1. Introduction

Dimple is one of the most effective structures for heat transfer enhancement in the industrial applications, such as the cooling of gas turbine blade and high pressure disk, the cooling of microelectronic components, and automotive, heating and refrigerating. Although these approaches are the effective method to improve the heat transfer performance; however, the increasing of fluid stream pressure drop should be concerned. The dimple surface is one of the effective methods to improve the heat transfer rates without significant pressure drop [1, 2]. Normally, the dimpled surface generates the vortex flow within its hole and the argumentation of heat transfer is obtained.

In past decades, lots of efforts have been made to improve efficiency and performance of thermal equipment accompanying a reduction in their size, weight and cost. The heat transfer can be enhanced by using either active and/or passive techniques. There are multifarious passive techniques such as swirl flow devices [3], surface tension devices, rough surfaces [3, 4], pin fins [3], ribbed tabulators [3] and surfaces with dimple [5, 6]. These are used for enhancing heat transfer in different utilizations. Dimple is regarded as one of the most effective heat transfer enhancement because of its profits for low pressure losses comparing with other devices and enhancing for heat transfer [7].

A wind tunnel investigation on an array of hemispherical dimple in staggered arrangement has been conducted by Manmood et al. [8]. In this work, they informed the formation of large vortexes pair on the dimple surface. Won et al. [9], Ligrani et al. [10], Won and Ligrani [11] and Shin Et al. [12] have reported about flow structure of dimple.

Previous studies, a CFD technique has been carried out popularly to investigate flow and heat transfer of dimple array in channel flow because of more accurate prediction of results by adopting of excellent turbulence model. Rao et al. [5] studied the flow and heat transfer of hemispherical and tear drop dimples by using CFD technique. The dimensions of hemispherical dimples were similar to the case of Mahmood et al. [8]. The results have been reported the heat transfer characteristics on the dimple surface in detail and proved CFD and experimental results for measuring overall heat transfer. Moreover, flow and heat transfer of dimple array in channel flow was investigated by Kim and Shin [13], Yoon et al. [14], Elyyan et al. [15] Xie et al. [7] using CFD technique. To reduce calculation load for computational modelling, the evaluated area of heat transfer was applied on some parts of dimple array.

The flow and heat transfer characteristics of teardrop dimple and protrusion was investigated and compared with hemispherical dimple and protrusion by Xie et al. [7]. They showed the thermal performance for teardrop dimple and protrusion is higher than hemispherical dimple and protrusion for lower Reynolds number and thermal performance increase gradually as the centre moves downwards for the teardrop dimple/protrusion.

Therefore, many researchers have been studied about different shapes shuch as spherical, teardrop and square shape [16] but conical shape have not been studied yet. Conical shape has many advantag for forming or creating easier than spherical or tear-drop shape. In this work, heat transfer effects and flow characteristics on a surface of conical dimple were investigated. Single row of conical dimples were designed over the internal surface of wind tunnel. The wind tunnel was arranged to get enough fully developed flow. Computational Fluid Dynamic (CFD) was used to visualize flow characteristics of dimples and compare with some experimental results.

2. Method

2.1. Model of dimple

The model of conical dimple row was formed over the inner bottom surface of the rectangular wind tunnel as shown in figure 1. The air with fully developed flow passed through the test section. The origin of Cartesian coordinate system was existed at the centre of middle dimple. X-axis is the along the flow direction of wind tunnel, Y-axis is the rectangular wind tunnel height direction and Z-axis is normal direction to the flow.

Figure 2 shows the details of conical dimple with projected diameter was D=26.4 mm. The depth of dimple, from the surface to the dimple bottom tip, was 0.2D [5,13 and 17]. The spacing of dimple-to-dimple was adjusted at S=1.125D, 1.25D, 1.5D and 2D. The Reynolds number of air inside the wind tunnel is Re_H=20,000 that was based on the hydraulic diameter of wind tunnel [5,8].

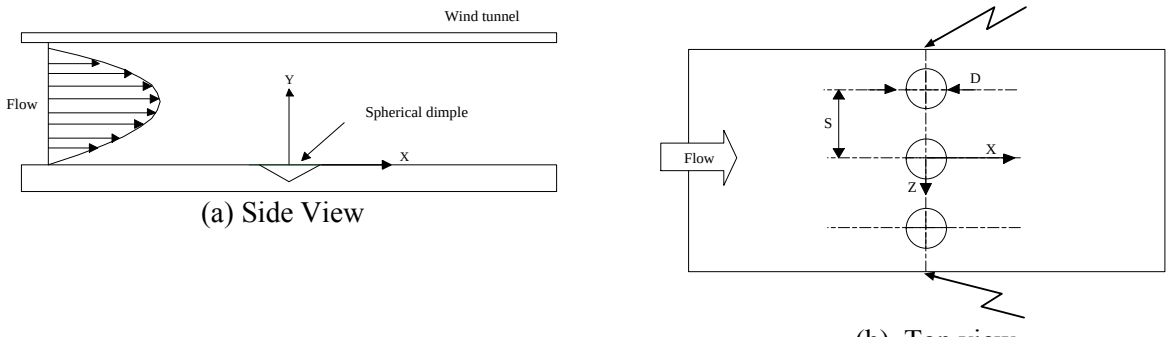

Figure 1. The model of investigation

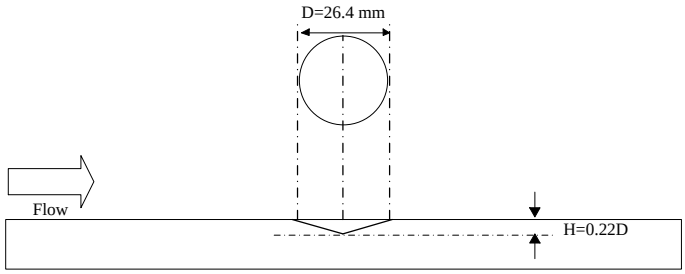

Figure 2. The details of dimple

2.2. Wind tunnel

The experimental setting for wind tunnel was utilized to prove and compare with CFD results. By using TLC technique, the heat transfer and temperature on the surface of smooth wall test section was measured. The wind tunnel measurement details were explained in previous works of M. Wae-Hayee et al. [18, 19]. The schematic diagram of wind tunnel simulation model was shown in figure 3. The wind tunnel geometries and dimensions for simulation were identical with the experimental design. The rectangular wind tunnel has three parts: the upstream of test section (1700 mm) that was sufficient distance to get fully developed flow, test section (280mm) where was formed conical dimples and downstream of test section where the air vent from the wind tunnel. The wind tunnel height was 26.4 mm (1D). The width of wind tunnel was varied with the spacing of dimple-to-dimple to reduce moderate computational loads of simulations.

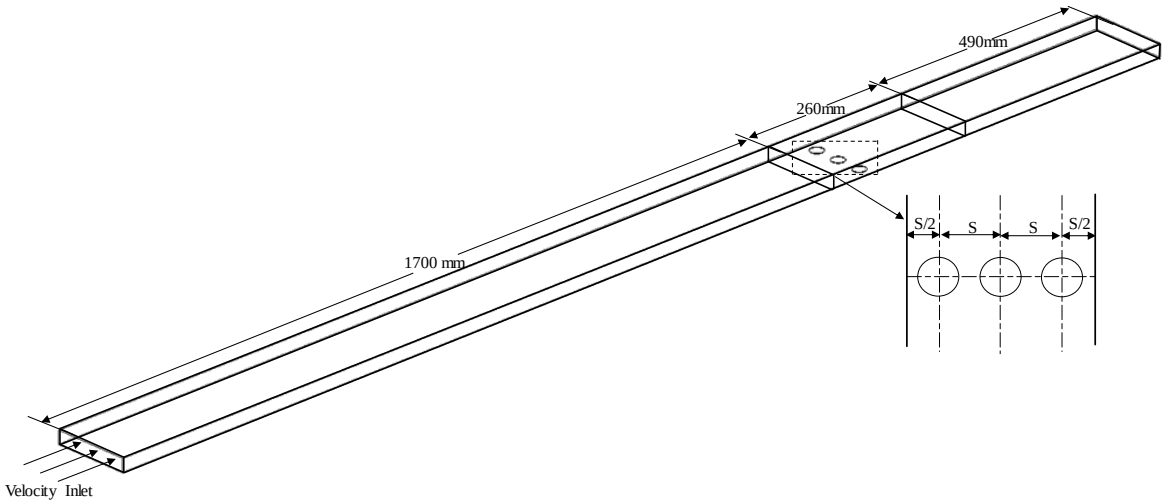

Figure 3. The wind tunnel with conical dimple

The generated grid details used in this work were illustrated in figure 4. Cutting plane along centreline of dimple was shown to expose the internal grid system. The majority of mesh elements were even rectangular. Uneven square elements were composed of dimple area and their surrounding regions. The elements were concentrated near the wall. Grid dependency in space between upper and lower wall is very important, especially, the thickness of the first layer above the wall to resolve the flow field within the viscous sublayer. To consider grid dependence in this work, y+ distributions on the heat transfer surface were lesser that 1. The selected element was 7,294,941 elements.

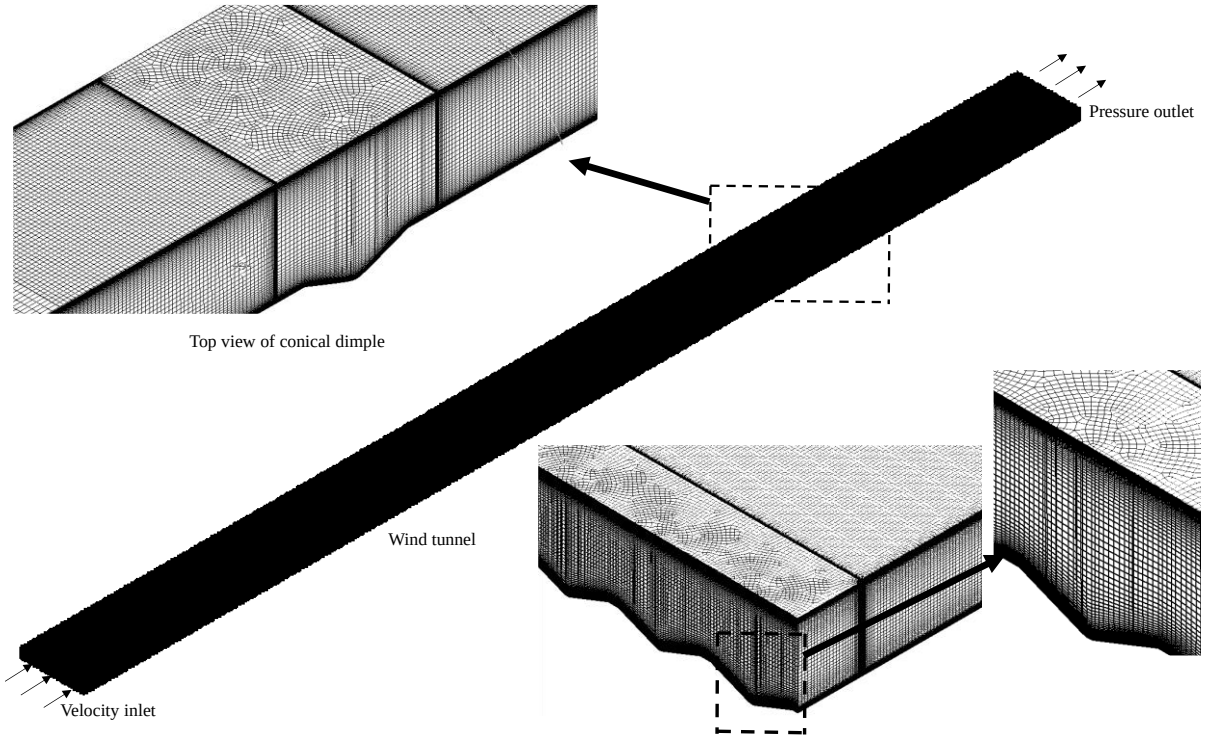

Figure 4. Generated grids

2.3. Assumptions and boundary conditions

In numerical model, the upper and the lower wall were set to have no slip condition. All walls, except bottom wall of test section, were insulated for performing as adiabatic condition. The fluid was considered as an incompressible flow with constant thermal properties and there is no gravitational effect in this simulation. At the air inlet, the uniform velocity was entered by getting Reynolds number at Re_H=20,000. The pressure outlet was set at 1 atm. Both of lateral walls were set as symmetry with the temperature of air was at 25°C. At the heat transfer surface formed with dimples was set at constant heat flux (150 W/m^2).

2.4. Numerical calculation method

The numerical 3-D model which based on the finite volume method was adopted to solve governing equations with boundary conditions. The details of equation can be found in [20]. The fluid flow and heat transfer were solved using a Shear Stress Transport (SST) k-ω turbulence model due to accurate prediction with moderate computation cost [20]. This turbulence model had been used in relative studies [5, 7 and 18].

The solution method was based on Semi-Implicit Method for Pressure-Linked Equations (SIMPLE) algorithm with second order upwind for all spatial discretization. To consider solutions to be convergent, the root mean square (RMS) residual of continuity and energy equation were lesser than 10^{-8} and that of momentum equation was lesser than 10^{-5} [5, 18].

2.5. Nusselt number calculation

The heat transfer coefficient, h, could be calculated from:

$$h = \frac{\dot{q}}{T_{wall} - T_{air}} \tag{1}$$

Where, $\dot{q}$ was heat flux, T_{wall} was wall temperature and T_{air} was air temperature.

The Nusselt number, *Nu*, was calculated from:

$$Nu = \frac{hD_H}{k} \tag{2}$$

where D_H was the hydraulic diameter of the tunnel and *k* was a thermal conductivity of the air.

3. Result and discussions

3.1. Verification of simulation

The well-known Dittus-Boelter correlation, $Nu_o = 0.23\,\mathrm{Re}^{0.8}\,\mathrm{Pr}^{0.4}$ where *Re* and *Pr* are Reynolds number and Prandtl number, were used for comparing internal heat transfer in the smooth channel. The average Nusselt numbers versus Reynold numbers for smooth wind tunnel was compared between the correlation, the experimental results, and the CFD method from this work is shown in figure 5. The current data agrees well with the correlation and the experimental results and overall heat transfer increase according to increasing of Reynolds number. The discrepancies of comparison were found in the same range with the work of Rao et al. [5].

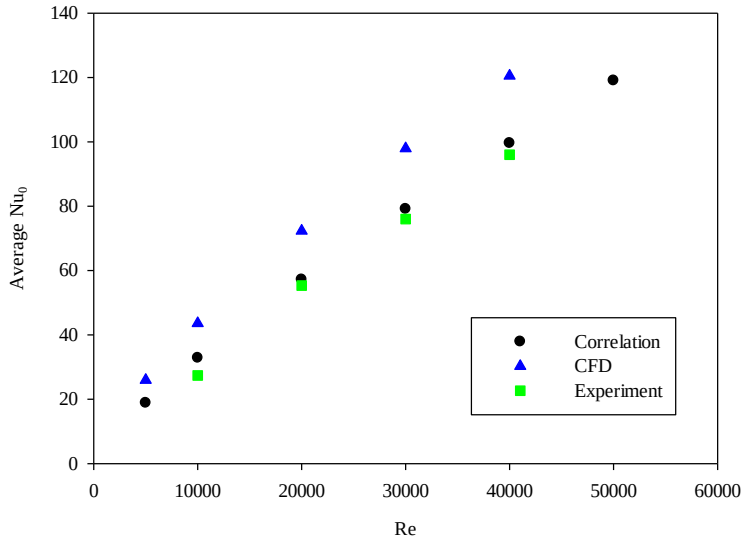

Figure 5. Average Nusselt numbers versus Reynold numbers of internal heat transfer correlation and the CFD method in this work

3.2. Flow characteristics

Streamlines flow over dimple surface were shown in figure 7. The occurrence of circulation flow in the dimple cavity was described obviously at the upstream part of the dimple cavity. The streamline inside the dimple cavity was shown in figure 6. This figure could also be proved that the circulation flows were happened at upstream half of the dimple cavity. The static circulation flow acted as thermal insulator resulting in low heat transfer on upstream portion of dimple surface.

For the case of 1.125D, the streamline which pass through the centre of middle dimple cavity (Z/D=0) where the flow condition inside the dimple was shown in figure 6. The stationary circulation flow appeared in upstream portion of dimple and attachment flow appeared in downstream portion of

dimple. This effect enhances heat transfer augmentation which had been described in literature reviews.

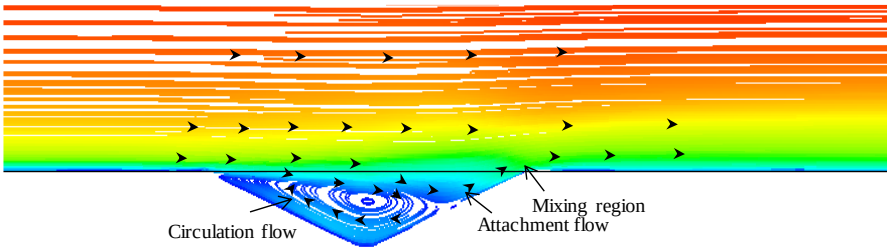

Figure 6. Streamline at the centre of plan of middle dimple (S/D=1.125D, Re=20,000).

In figure 7, the characteristics of upstream streamline (before passing dimple) were straight whereas those of downstream streamline (immediately after passing dimple, X/D≈0.5) were separated from its centre- line and tend to lateral side. This is from the effect of the longitudinal vortex pair occurrence after flow passing dimple which had also been reported in the literatures [5,7 and 23]. Here, it can be noted that for the case of S/D=1.125D as shown in figure 7 (a), the flow tendency to lateral sides of this vortex pair seems to be slighter than those other cases due to confinement from near neighbouring vortex pair in condition of short dimple-to-dimple spacing.

The conditions of the contour of Nusselt number on the surface of test section were illustrated in figure 8. High distribution of Nusselt number can be seen at the downstream portion of dimple cavity due to the attachment flow especially near the rear rim of dimples that was previously described in figure 6. But low Nusselt number distribution can be found at the upstream portion of dimple cavity because of stationary circulation flow. Increasing or decreasing Nusselt number on the dimple surface can be caused because of both attachment and circulation flow effects that was also studied in literature [5,7]. For all case, the Nusselt number distribution on the surface of smooth wall along downstream of every dimple have one peak for X/D=0.5 case and other X/D cases have two peak regions that was caused by the longitudinal vortex pair effect resulting in stronger circulating over the heat transfer surface of test section of wind tunnel. Simultaneously, these double peak regions area can be found along the downstream of smooth surface and this effect can remove more heat.

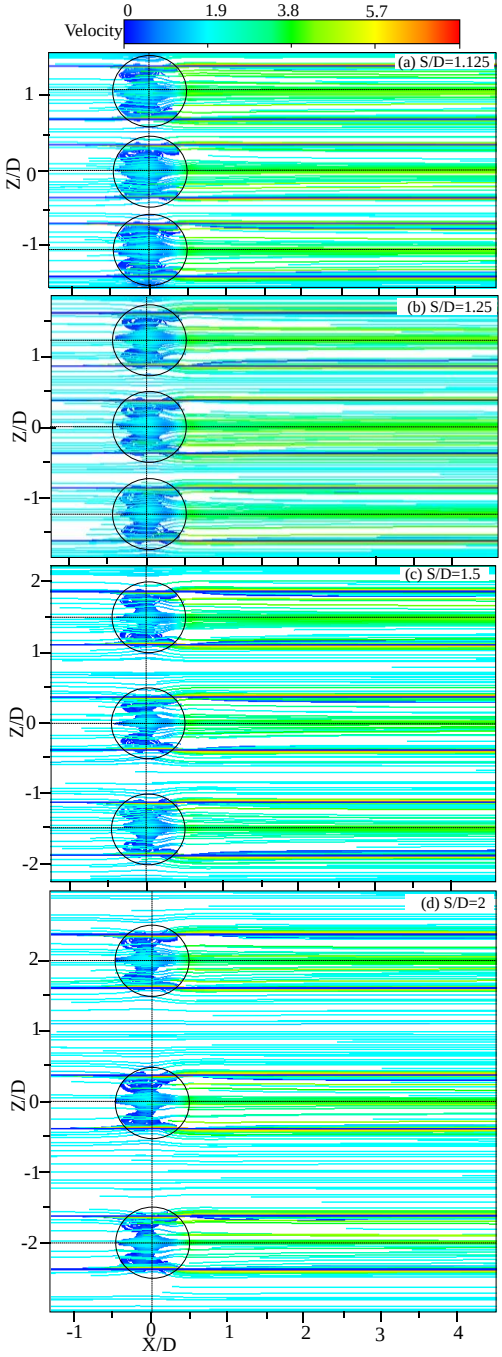

Figure 7. Streamline above the surface of dimples.

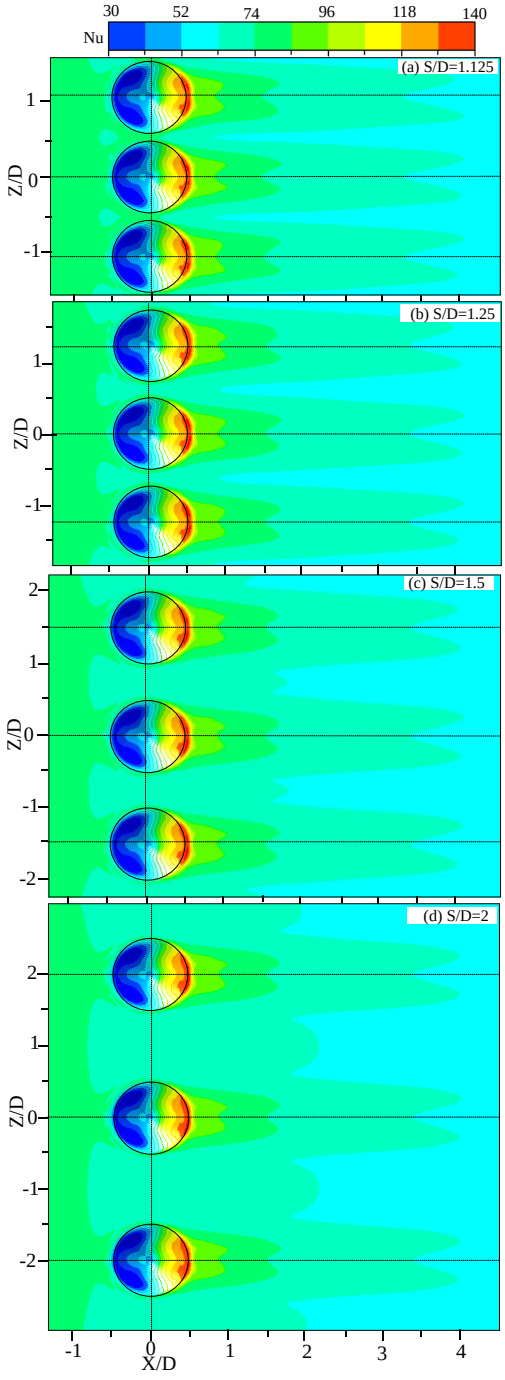

Figure 8. Nusselt number distributions on the surface (Re_H=20,000).

Span wise direction of Nusselt number distributions was shown in figure 9. Commonly for all S/D cases, high Nusselt number can be observed at just downstream of dimple cavity and became lower and lower along the direction of downstream. For every S/D cases, the single peak regions at every X/D=0.5 were extremely high and area of these peak regions were large because of the effect of attachment flow and double peak regions that was caused by the effect of neighbouring vortex pair between spacing

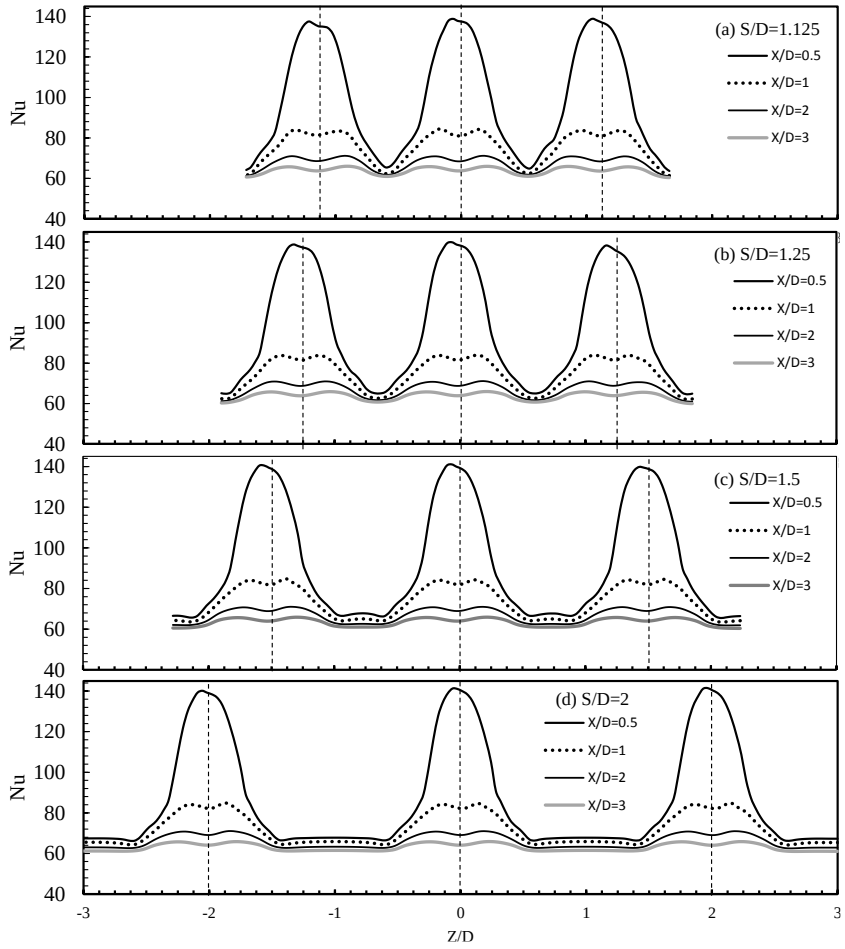

Figure 9. Nusselt number distributions in span wise direction (Dash straight line is the centre of dimple)

The average Nusselt number comparison for smooth and dimple surface was shown in figure 10. Every dimple surface's average value was higher than smooth surface. The trend of average Nusselt number became lower and lower when the spacing became larger and larger but the values were the same for S/D=1.25 and 1.5 cases.

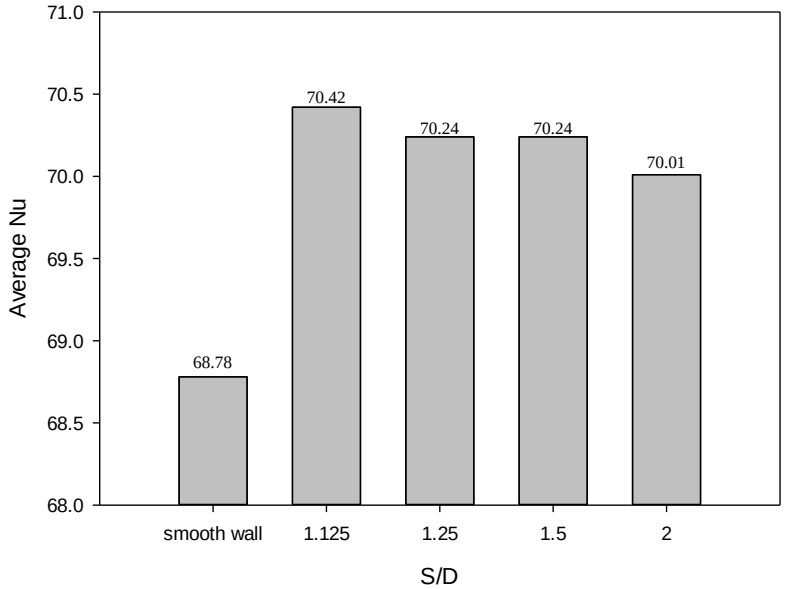

Figure 10. Comparison of Average Nusselt number for spherical and conical dimple

4. Conclusions

In this work, investigation of flow structure and heat transfer over the test section of wind tunnel for conical case that was adjusted by different spacings ($1.125 \leq S/D \leq 2$). The conclusions of this work are described as follow.

1. High Nusselt number regions were observed at the attachment flow region. At this place, the Nusselt number value are over 140.
2. Along the downstream of dimple, the pattern of Nusselt number was found into two peak regions ($X/D > 0.5$) for all S/D case.
3. The flow for $S/D = 1.125$ case, the circulation flow was seemed to be stronger than other cases. This effect can enhance heat transfer.
4. For the Nusselt number average, the dimple surfaces were higher than smooth surface. Moreover, the trend of average Nusselt number was lower when the spacing was increased.

Acknowledgement

The research grant was supported by the Research and Development Office (RDO), Prince of Songkla University, grant No. ENG590725S.

References

[1] Heo S C, Seo Y H, Ku T W and Kang B S 2011 Formability evaluation of dimple forming process based on numerical and experimental approach *J. Mech. Sci. Technol.* **25** 429–439
[2] Lan J, Xie Y and Zhang D 2011 Effect of leading edge boundary layer thickness on dimple flow structure and separation control *J. Mech. Sci. Technol.* **25** 3243–51
[3] Ligrani P M, Oliveira M M and Blaskovich T 2003 Comparison of heat transfer augmentation techniques *AIAA J.* **41** 337–362
[4] Kurniawan R, Kiswanto G and Ko T J 2017 Surface roughness of two-frequency elliptical vibration texturing (TFEVT) method for micro-dimple pattern process *Int. J. Mach. Tools Manuf.* **116** 77–95
[5] Rao Y, Li B and Feng Y 2015 Heat transfer of turbulent flow over surfaces with spherical dimples and teardrop dimples *Exp. Therm. Fluid Sci.* **61** 201–209

[6] Vorayos N, Katkhaw N, Kiatsiriroat T and Nuntaphan A 2016 Heat transfer behavior of flat plate having spherical dimpled surfaces *Case Stud. Therm. Eng*. **8** 370–377
[7] Xie Y, Qu H and Zhang D 2015 Numerical investigation of flow and heat transfer in rectangular channel with teardrop dimple/protrusion *Int. J. Heat Mass Transf.* **84** 486–496
[8] Mahmood G I, Hill M L, Nelson D L, Ligrani P M, Moon H K and Glezer B 2000 Local Heat Transfer and Flow Structure on and Above a Dimpled Surface in a Channel *J. Turbomach.* **123** 115–123
[9] Won S Y, Zhang Q and Ligrani P M 2005 Comparisons of flow structure above dimpled surfaces with different dimple depths in a channel *Phys. Fluids* **17** 0451051–9
[10] Ligrani P M, Harrison J L, Mahmmod G I and Hill M L 2001 Flow structure due to dimple depressions on a channel surface *Phys. Fluids* **13** 3442–51
[11] Won S Y and Ligrani P M 2007 Flow characteristics along and above dimpled surfaces with three different dimple depths within a channel *J. Mech. Sci. Technol.* **21** 1901–09
[12] Shin S, Lee K S, Park S D and Kwak J S 2009 Measurement of the heat transfer coefficient in the dimpled channel: effects of dimple arrangement and channel height *J. Mech. Sci. Technol.* **23** 624–630
[13] Kim K Y and Shin D Y 2008 Optimization of a staggered dimpled surface in a cooling channel using Kriging Model *Int. J. Therm. Sci.* **47** 1464–72
[14] Yoon H S, Park S H, Choi C and Ha M Y 2015 Numerical study on characteristics of flow and heat transfer in a cooling passage with a tear-drop dimple surface *Int. J. Therm. Sci.* **89** 121–135
[15] Elyyan M A and Tafi D K 2008 Large eddy simulation investigation of flow and heat transfer in a channel with dimples and protrusions *J. Turbomach.* **130** 0410161–9
[16] Acharya S and Zhou F 2012 Experimental and computational study of heat/mass transfer and flow structure for four dimple shapes in square internal passage *J. Turbomach.* **134** 0610281–13
[17] Isaev S A, Schelchkov A V, Leontiev A I, Baranov P A and Gulcova M E 2016 Numerical simulation of the turbulent air flow in the narrow channel with a heated wall and a spherical dimple placed on it for vortex heat transfer enhancement depending on the dimple depth *Int. J. Heat Mass Transf.* **94** 426–448
[18] Wae-Hayee M, Tekasakul P, Eiamsaard S and Nuntadusit C 2015 Flow and heat transfer characteristics of in-line impinging jets with cross-flow at short jet-to-plate distance *Experimental Heat Transf*er. **28** 511–530
[19] Wae-Hayee M, Tekasakul P, Eiamsaard S and Nuntadusit C 2014 Effect of cross-flow velocity on flow and heat transfer characteristics of impinging jet with low jet-to-plate distance *J. Mech. Sci. Technol.* **28** 2909–17
[20] Versteeg H K and Malalasekera W 2007 *An Introduction to Computational Fluid Dynamics*, Second Edition, Pearson Prentice Hall
[21] Mahmood G I and Ligrani P M 2002 Heat transfer in a dimpled channel: combined influences of aspect ratio, temperature ratio, Reynolds number, and flow structure *Int. J. Heat Mass Transf.* **45** 2011–20